Journal of Engineering Physics and Thermophysics, Vol. 83, No. 6, 2010

EXPLOSION GENERATION OF MICROATOMIZED LIQUID-DROP AEROSOLS AND THEIR EVOLUTION

B. I. Vorozhtsov, O. B. Kudryashova, A. N. Ishmatov,
I. R. Akhmadeev, and G. V. Sakovich

UDC 621.45.042:532.592.2:544.772

The formation of a microatomized aerosol was investigated with the use of a model of an explosion atomizer based on a hydrodynamic shock tube with atomization through a clearance (nozzle). It is shown that the cavitation of the liquid subjected to atomization plays a great role in the production of a microatomized liquid-drop aerosol. A mathematical model describing the genesis of an aerosol cloud is proposed. The time of propagation of a compression wave in the liquid subjected to atomization and the time of its outflow from the atomizer were estimated, the size distribution of the aerosol particles was constructed, and the dependence of this distribution on the coagulation, evaporation, and precipitation of the aerosol particles was determined. A technique for undisturbed measurement of the genesis of an aerosol is described. Results of an experimental investigation of the dispersion parameters of an aerosol and the processes of formation and propagation of an aerosol cloud produced as a result of the explosion atomization of a liquid are presented.

Keywords: *aerosol, atomization, coagulation, evaporation, precipitation, cavitation, explosion.*

Introduction. In a number of applications, it is necessary to rapidly introduce a microatomized aerosol into any zone that can be difficult to reach. Among these applications are:

1) the absorption of toxic substances, the disinfection of rooms, the anti-microbial treatment of objects;
2) weapons of nonlethal action in peacemaking operations (aerosols bringing people to a stop, e.g., with the use of pepper spray) [1];
3) the suppression of fire in vehicles or in production floor areas, the liquidation of ignition sites in cable ducts;
4) inhalation in medicine and veterinary medicine, improvement of the techniques for carrying aerosols to the lungs of patients [2];
5) the production of protection and camouflage screens, etc. [3].

In this case, the higher the dispersity of the aerosols, the better the effect achieved with them because the larger the specific mass surface of the drop volume of an aerosol, the larger the total area of evaporation of its small drops, which increases the rate of action of the chemical agents. For example, aerosol medicines, considered as an alternative to those introduced into the organisms of people and animals by invasive and peroral methods, precipitate in the alveolar part of the lungs much better in the case where the characteristic size of their drops comprises only several tens of nanometers [2]. Thus, of great practical importance are aerosols consisting of particles with characteristic sizes of the order of one micron or smaller, and in a number of applications it is necessary to rapidly (instantaneously) obtain such aerosols with no changes in the physicochemical properties of the dispersed substances. To this point this problem has not been solved. The rate of production of an aerosol is of prime importance in the case where this aerosol is used for the completion of collective means of protection against unhealthy and dangerous substances in civil defense or in industrial safety, as well as in the case where it is used in fire-fighting equipment.

It is precisely the explosion method that makes it possible to produce aerosols with a high rate. The method of explosion atomization used in practice has been much studied [4, 5]. However, up till now the problem on the production of aerosols with submicron sizes has not been posed and, correspondingly, such aerosols have not been ob-

---

Institute of Problems of Chemical and Power Technologies, Siberian Branch of the Russian Academy of Sciences, Sotsialisticheskaya Str., Biisk, Altaiskii Krai, 659322, Russia; email: olgakudr@inbox.ru. Translated from Inzhenerno-Fizicheskii Zhurnal, Vol. 83, No. 6, pp. 1084–1103, November–December, 2010. Original article submitted April 20, 2010.

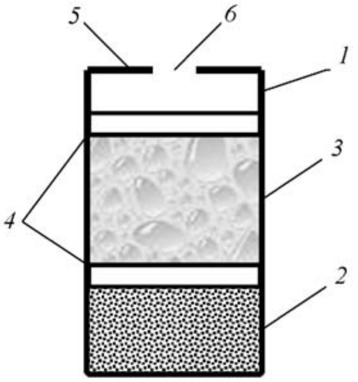

Fig. 1. Diagram of an explosion atomizer.

tained, despite the need for the above-described applications of them. In this connection, we have developed a special explosion atomizer for obtaining micron and submicron aerosols.

The present work is devoted to theoretical and experimental investigation of the generation of liquid-drop aerosols with the use of the newly designed explosion atomizer and the process of their further evolution. The measurements were carried out with the use of a complex of special means, including contactless ones, making possible measurements with no sampling and causing no changes in the structure of a substance. An analysis of the experimental data obtained allowed us to determine the degree of dispersion of the liquids being investigated.

Despite the fact that the kinetics of aerosol clouds has been investigated over many decades, the processes occurring in a liquid-drop aerosol are still imperfectly understood. In our opinion, it is most difficult to describe the dynamics of a microatomized cloud because, in this case, it is necessary to simultaneously take into account the rapid evaporation of submicron drops due to the curvature of their surface and the precipitation and coagulation of aerosol particles as well as the influence of the atmospheric humidity, the physicochemical properties of the atomized liquid, and the environment. The physical and mathematical model proposed in the present work allows one to estimate the indicated effects and to determine the dependence of the dispersion parameters of an aerosol on time, the physicochemical characteristics of the liquid atomized, and the conditions of its atomization, which is not only of theoretical interest but is important for the production of aerosols with required dispersion characteristics.

1. Mathematical Model of Explosion Generation of Microatomized Aerosols. *1.1. The first stage of the process — the detonation of an explosive.* The atomizer developed represents a modified water tunnel (Fig. 1). It comprises body 1, in which an explosive charge 2 and liquid 3, the volume of which is bounded by membrane 4, are placed.

The liquid is ejected through clearance 6, the width of which is limited by the edges of the body and reflector 5. The volume of the explosion chamber is equal to V_1. When explosive 2 detonates in the volume V_1 within a time of the order of one microsecond, this volume is filled with gases under a pressure of several hundreds of atmospheres. These gases exert a high-power pulsed action on the liquid and, in doing so, give rise to a shock wave in it. The reflector and the fairly wide clearance (nozzle) provide a gradual outflow of the liquid due to the piston ejection of it and keep the gases formed as a result of the explosion from the break-through. On the other hand, the liquid is completely expelled in this case.

The problem on the propagation of a shock wave in a closed volume is substantially complicated by the reflection and refraction of this wave, especially in the case where it passes from one medium to another, and the strength properties of the medium impose restrictions on the solution of the problem. For the case being considered, of importance is the bubble cavitation of the liquid [5, 6]. It will be shown below that, even though this phenomenon is difficult to consider, it is very useful for the formation of a microatomized liquid-drop aerosol.

To investigate the processes of propagation of a shock wave in a liquid subjected to atomization in the atomizer proposed, we will simulate these processes with the use of the phenomenological laws of wave motion in such an apparatus. The problem will be solved in the acoustic approximation because the shock wave formed in the indicated apparatus experiences one or two reflection cycles and degenerates rapidly into the acoustic wave, and it is precisely these conditions under which a cavitation zone is formed. Below is a brief description of the mathematical model used [7].

The maximum pressure p_m in the shock wave formed under the above-described conditions is determined by the pressure of the gases formed in the explosion chamber of volume V_1. Let us determine this pressure.

The detonation of an explosive in the explosion chamber of volume V_1 represents an isochoric process: V_1 = const. In this case, the gas does no work, and the energy of the explosion transformation of the explosive Q increases its internal energy, i.e.,

$$Q = \Delta U = c_v m_g \Delta T . \tag{1}$$

The temperature of the gas released as a result of the explosion will be equal, in accordance with (1), to

$$T_g = \frac{Q}{c_v m_g} + T_1 , \tag{2}$$

where T_1 is the initial temperature in the explosion chamber.

In the case of an instantaneous detonation, the gas pressure will be equal to

$$p_m = \frac{\gamma - 1}{\gamma} \frac{Q}{V_1} . \tag{3}$$

Let us estimate the temperature and pressure of the gas in the explosion chamber of the atomizer being considered immediately after the detonation of the explosive used. The pressure is transferred through the membrane to the liquid column and gives rise to a shock wave with amplitude p_m; this wave can be considered as an acoustic wave in the first approximation.

We now write the main expressions relating the energy of the explosive charge to the maximum displacement of the liquid particles Z_m, accounting for the reflection of the shock wave. It will be assumed that the velocity of propagation of the wave in the liquid is equal to the velocity of sound c.

The intensity of the wave field, i.e., the energy falling on the surface S_1 during the time t, will be determined as

$$I = \frac{Q}{t S_1} . \tag{4}$$

From the known relations for the wave processes it follows that

$$I = \frac{\rho_{liq} Z_m^2 \omega^2 c}{2} .$$

Using this expression and expression (4), we write an expression for the maximum displacement of liquid particles in the shock wave:

$$Z_m = \sqrt{\frac{2Q}{t \rho_{liq} S_1 \omega^2 c}} . \tag{5}$$

The time it takes for the shock wave to reach the opposite surface of the liquid is equal to

$$t_w = \frac{L}{c} . \tag{6}$$

Since the shock wave is completely reflected from the surface of the liquid at its boundary with the air (the reflection coefficient $\frac{\rho_{liq} c - \rho_0 c_0}{\rho_{liq} c + \rho_0 c_0} = 0.9988 \approx 1$), vibrations with a wavelength $\lambda = 2L$ arise in the liquid layer. The frequency of these vibrations is equal to

$$\omega = \frac{\pi c}{L}. \tag{7}$$

Such wave parameters are characteristic of both the compression wave and the reflected wave because the reflection coefficient is close to unity. Since the shock wave is reflected from the boundary between the liquid and the air, a wave with the opposite phase, i.e., an expansion wave, propagates to the liquid.

From (5), with the use of (6), (7) and the expression for the mass of the liquid subjected to atomization $M_{\text{liq}} = LS_1\rho_{\text{liq}}$, we obtain the dimensionless parameter

$$\frac{Z_{\text{m}}}{L} = \frac{1}{\pi c}\sqrt{\frac{2Q}{M_{\text{liq}}}}, \tag{8}$$

characterizing the efficiency of the cavitation processes — the value of the plane discontinuity in relation to the height of the liquid column. This parameter is primarily determined by the energy of the explosive in relation to the mass of the liquid: the larger the ratio between these quantities, the higher the cavitation efficiency. If this parameter is small, the cavitation processes can be disregarded in the problem.

1.2. Development of the liquid cavitation. When particles of the liquid subjected to atomization displace by a maximum distance Z_{m} under the action of the unloading wave (in the expansion phase), a discontinuity appears and the liquid evaporates into this void. In the next compression phase, a ball-like bubble of diameter D_1 filled with water vapor is formed in the water.

It may be suggested that a plane rarefaction wave gives rise to a plane discontinuity with an effective thickness $Z_{\text{ef}} = \frac{Z_{\text{m}}}{\sqrt{2}}$. In this discontinuity, we separate an element with a characteristic size Z_{ef}. The number of such elements is $N = \frac{S_1}{Z_{\text{ef}}^2}$; they are filled partially with water and partially with water vapor, and their density comprises about $0.8\rho_{\text{liq}}$ [5]. This corresponds to the cavitation index $k = V_{\text{liq}}/V_{\text{el}} \approx 0.8$. The volume of such an element $V_{\text{el}} \sim Z_{\text{ef}}^3$. For it, $D_1^3 = (1-k)Z_{\text{ef}}^3$.

The process of expansion of a cavitation bubble is adiabatic; therefore,

$$p_{\text{m}}\left((1-k)\,Z_{\text{ef}}\right)^{3\gamma} = pD_1^{3\gamma}, \tag{9}$$

hence

$$D_1 = \frac{L(1-k)}{\pi c}\sqrt{\frac{Q}{M_{\text{liq}}}}\sqrt[3\gamma]{\frac{p_{\text{m}}}{p}}. \tag{10}$$

The vapor-water mixture representing a water frame with cavitation bubbles distributed in it is ejected through the atomizer clearance in the form of a plane flow of thickness exceeding Z_{ef} by 2–3 times under the pressure due to the further expansion of the explosive-detonation products. The velocity of movement of this mixture through the clearance depends on the pressure in the chamber; this pressure decreases with decrease in the flow rate of the liquid. On the other hand, the size of the bubbles increases with decrease in the pressure (10). Thus, each unit liquid volume contains inclusions, the size of which is determined by the pressure, disturbing the liquid flow continuity.

To estimate the minimum diameter of the liquid particles and determine its dependence on the parameters of the system, we write relations for the velocity of the liquid flow with the use of the continuity equation

$$S_1u_1 = S_2u \tag{11}$$

and the Bernoulli equation

$$p + \frac{k\rho_{\text{liq}}}{2} u_1^2 = p_0 + \frac{k\rho_{\text{liq}}}{2} u^2 , \tag{12}$$

from which follow relations for the velocities of movement of the vapor-water mixture inside the system and on the surface of the clearance:

$$u_1 = \sqrt{\frac{p - p_0}{\frac{k\rho_{\text{liq}}}{2} ((S_1/S_2)^2 - 1)}} , \tag{13}$$

$$u = \frac{S_1}{S_2} \sqrt{\frac{p - p_0}{\frac{k\rho_{\text{liq}}}{2} ((S_1/S_2)^2 - 1)}} . \tag{14}$$

We now determine how the pressure in the explosion chamber changes. Up to the termination of the liquid outflow, this pressure changes only due to the increase in the free volume as a result of the outflow of the liquid:

$$pV = p_{\text{m}} S_1 L = \text{const} . \tag{15}$$

The rate of change in the volume of the liquid due to its outflow is determined by the relation

$$\frac{dV}{dt} = uS_2 . \tag{16}$$

Since in the process of pressing-out of the liquid the conditions are such that the pressure in the apparatus is much higher than the atmospheric pressure, $p >> p_{\text{a}}$, the velocity of the liquid outflow can be calculated fairly exactly by the equation

$$u = \frac{S_1}{S_2} \sqrt{\frac{p}{\frac{k\rho_{\text{liq}}}{2} ((S_1/S_2)^2 - 1)}} . \tag{17}$$

It follows from (16) and (17) that

$$\frac{dp}{dt} = -\frac{1}{p_{\text{m}} L} \sqrt{\frac{p}{\frac{k\rho_{\text{liq}}}{2} ((S_1/S_2)^2 - 1)}} \, p^2 . \tag{18}$$

Integration of this equation gives the relation defining the change in pressure inside the explosion chamber depending on the time of the liquid outflow:

$$p = p_{\text{m}} \left[1 + t \frac{3}{\sqrt{2}\, L} \sqrt{\frac{p_{\text{m}}}{k\rho_{\text{liq}} ((S_1/S_2)^2 - 1)}} \right]^{-2/3} . \tag{19}$$

Integrating (16) with the use of (17) and (15), we obtain the time of complete liquid outflow:

$$t_{\text{out}} = L^2 \frac{2}{3} \sqrt{\frac{2 p_{\text{m}}}{k\rho_{\text{liq}} ((S_1/S_2)^2 - 1)}} . \tag{20}$$

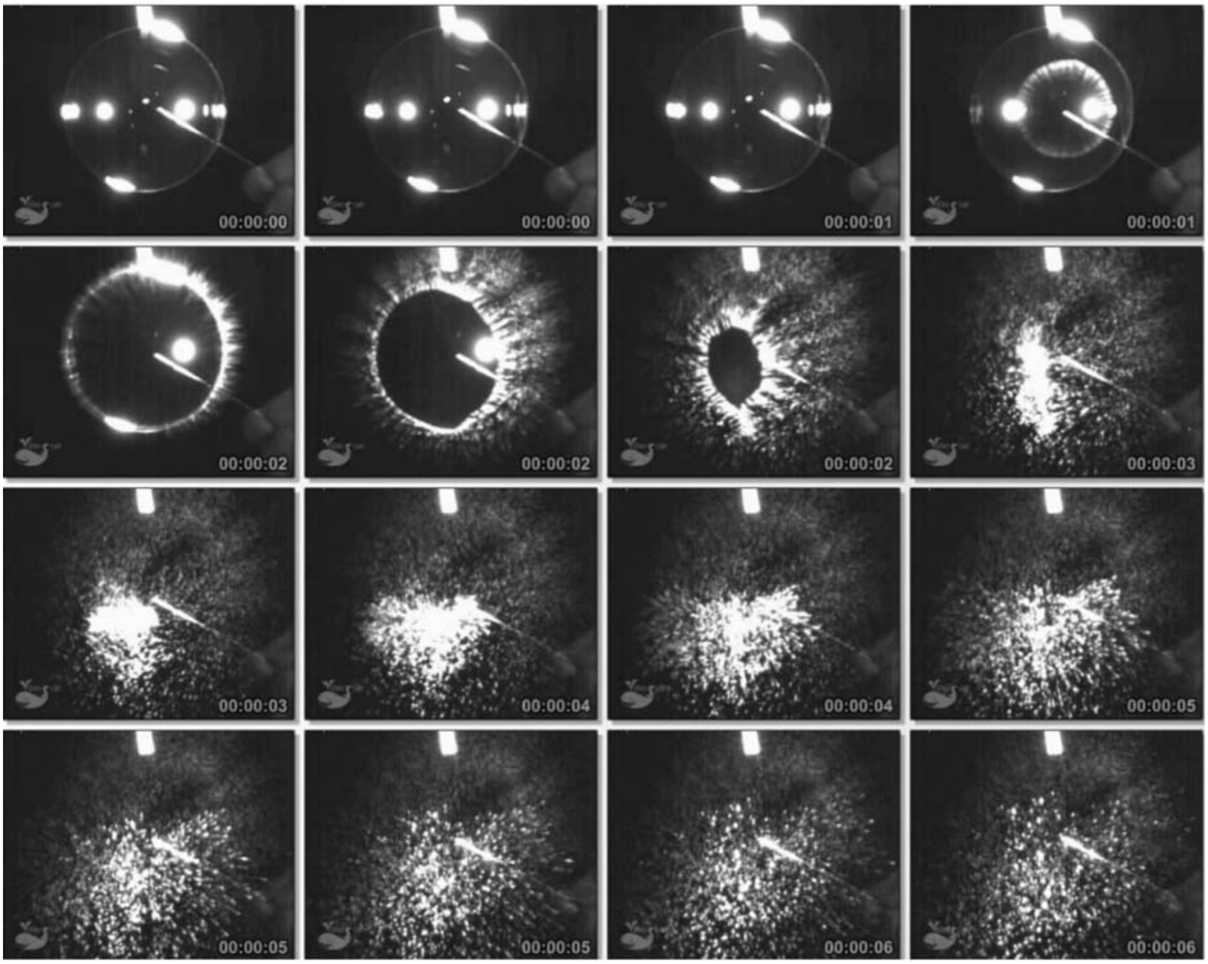

Fig. 2. Frames of a high-speed photography of the process of breakdown of a soap bubble.

The atomizer proposed with a reflector and a wide clearance (nozzle) provides, on the one hand, a gradual outflow of the liquid and, on the other, its piston pushing-out without the break-through of the gases formed as a result of the explosion.

The minimum pressure in the liquid is determined from expressions (19) and (20):

$$p_{\text{f}} = p_{\text{m}} \left(1 + \frac{2Lp_{\text{m}}}{k\rho_{\text{liq}} \left((S_1/S_2)^2 - 1 \right)} \right)^{-\frac{2}{3}} . \tag{21}$$

1.3. Breakdown of cavitation bubbles and formation of a microatomized aerosol. Particle-size distribution function. Thus, in the process of explosion atomization of a liquid in the atomizers proposed, cavitation bubbles are formed. The vapor-water mixture representing a water frame with cavitation bubbles distributed in it is ejected through the clearance (nozzle) of the atomizer under the pressure as a result of the further expansion of the explosive-detonation products in the explosion chamber. The velocity of the liquid flowing through the clearance depends on the pressure in this chamber, with decreases with decrease in the flow rate of the liquid. On the other hand, the size of the bubbles increases with decrease in the pressure in the explosion chamber (10). Thus, each unit liquid volume contains inclusions breaking up the continuity of the liquid flow, the size of which depends on the pressure.

We now determine the influence of the cavitation of the liquid on the formation of aerosol particles and on the mass concentration of the aerosol and find the size distribution function of the liquid particles.

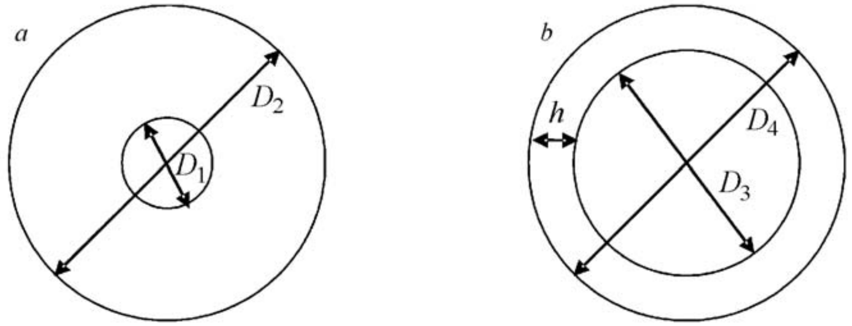

Fig. 3. Cavitation element prior to the liquid outflow (a) and after the outflow of the liquid from the atomizer clearance (b). D, h, μm.

The process of destruction of drops and bubbles is very complex and is characterized by the interaction of the surface-tension, viscous, and inertial forces. At present, there are a large number of works devoted to the investigation of the breaking up of individual drops and drop systems under different conditions of their interaction with a gas flow ([8] and the literature cited therein).

If it is assumed that each bubble found in the cavitation liquid under the pressure p blows out to the atmospheric pressure at the instant of ejection of this liquid and bursts at this instant with formation of drops with a diameter equal to the thickness of the water layer, the number of such drops can be estimated. Then the particle-size distribution function of the aerosol can be constructed on the basis of the data on the change in the pressure p with decrease in the flow rate of the liquid.

To support the assumption that a bubble breaks down into small drops with a diameter of the order of the thickness of the bubble wall, we present frames of a high-speed photography of the breaking of a soap bubble (Fig. 2). It is seen from the first frames that the bubble breaks down into approximately equal fragments with a diameter comparable with the thickness of the bubble wall.

Let us assume that the diameter of a cavitation element found in the liquid prior to its ejection from the clearance of the atomizer is equal to D_2, the diameter of this element after the ejection at the instant of its breakdown is D_4, and the diameter of the bubble under atmospheric pressure p_0 is D_3 (Fig. 3). We will consider the case of an instantaneous expansion of the bubble (the adiabatic process), where

$$\frac{D_3}{D_1} = \left(\frac{p}{p_0}\right)^{\frac{1}{3\gamma}}. \tag{22}$$

On condition that the volumes of the water in an element prior to and after the liquid ejection are equal, $D_2^3 - D_1^3 = D_4^3 - D_3^3$. The thickness of the water layer at the instant of breakdown of the element is equal to $h = (D_4 - D_3)/2$. Using (22), we obtain an expression for h:

$$h = \frac{D_1}{2}\left[\sqrt[3]{\frac{k}{1-k} + \left(\frac{p}{p_0}\right)^{1/\gamma}} - \left(\frac{p}{p_0}\right)^{1/3\gamma}\right]. \tag{23}$$

From expression (23), with the use of (10) we can determine the dependence of the thickness of the water wall of a bubble at the instant of its breakdown on the pressure in it.

The initial layer i of the vapor-gas mixture of area S_1 and thickness h is divided finally into n aerosol particles of diameter h ($n_i = \frac{6S_1}{\pi h^2}$), the number of which will decrease with each instant of time with increase in their diameter and decrease in the pressure. Let us introduce the relative number of particles $n_{\text{rel}} = n_i/\sum_{i=1}^{N} n_i$, where N is the number of liquid layers up to the instant the liquid outflow is completed. Calculating the number of ejected particles successively in each layer with account for the gradual decrease in the pressure from p_m to p_f, one can construct, with the use of (10), (19), (21), and (23), the dependence of the relative amount of particles on their sizes and then approximate the expression obtained by the distribution gamma function.

Microatomized-aerosol particles evaporate rapidly because of the curvature of their surface, which should be taken into account in the model. The dynamics of evaporation of small drops is determined by the Maxwell equation

$$I = \frac{dm}{dt} = \frac{4\pi r D_{\text{dif}} M (p_{\text{d}} - p_{\text{pl}})}{RT} , \tag{24}$$

where $r = h/2$. Integrating (24) with account for the initial conditions $r(0) = r_0$, we obtain

$$r^2 = r_0^2 - \frac{2MD}{RT\rho_{\text{liq}}} (p_{\text{d}} - p_{\text{pl}})\, t . \tag{25}$$

To estimate the partial pressure over the surface of a particle, we will use the Thomson (Kelvin) formula, determining the pressure of the saturated vapor over a liquid drop:

$$\ln (p_{\text{d}}/p_{\text{pl}}) = \frac{2\sigma M}{\rho_{\text{liq}} RTr} , \tag{26}$$

where σ is the coefficient of surface tension of the drop substance.

A liquid drop is completely evaporated when its radius $r = 0$ at the instant of time t. Thus, from (25) with the use (26) we obtain an expression for the lifetime of this drop:

$$t_1 = r_0^2 \Bigg/ \left[\frac{2MD_{\text{dif}} p_{\text{pl}}}{RT\rho_{\text{liq}}} \left(\exp\left(\frac{2\sigma M}{\rho_{\text{liq}} RTr_0} \right) - 1 \right) \right] . \tag{27}$$

1.4. Numerical estimates and discussion of calculation results. Let us perform numerical estimations and calculations with the use of the model proposed for description of the explosion genesis of a liquid-drop aerosol.

The parameters of the atomizer used are as follows: V_1 = 1 cm^3, the thickness of the liquid layer L = 1 cm, and the area of the cross section of the hydrodynamic tube S_1 = 1 cm^2. The explosive used possesses the following characteristics: Q = 50 kJ; γ = 1.3. In this case, according to (3), the maximum pressure of the liquid p_m = 11.5 MPa.

We now estimate, using (6), (7), and (8), the maximum displacement of the liquid particles in the atomizer with the above-indicated characteristics:

$$\omega = \frac{\pi \cdot 1500 \text{ m/s}}{10^{-2}\ \text{ì}} = 4.7 \cdot 10^5 \text{ Hz} ,$$

$$t_{\text{w}} = \frac{10^{-2} \text{ m}}{1500 \text{ m/s}} = 6.7 \cdot 10^{-6} \text{ s} ,$$

$$Z_{\text{m}} \approx 671\ \mu\text{m} .$$

The dimensionless parameter characterizing the efficiency of the cavitation process (8) has a value of about 0.067 in our case, and the maximum breakdown of the liquid comprises about 7% of the height of the liquid column. This is a fairly large value that points to the fact that the liquid cavitation is insignificant in the problem being considered.

We now estimate the velocity of a vapor-water mixture flow. Since $k \approx 0.8$ [5] and ρ_{liq} = 998 kg/m^3 (water), the velocities of this flow will have the following values at a maximum pressure in the explosion chamber of

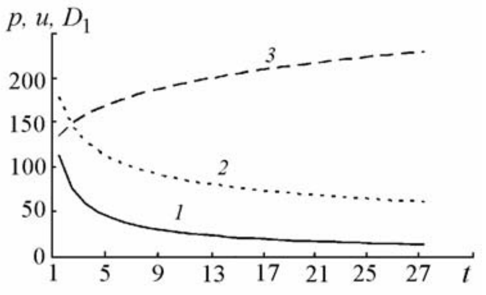

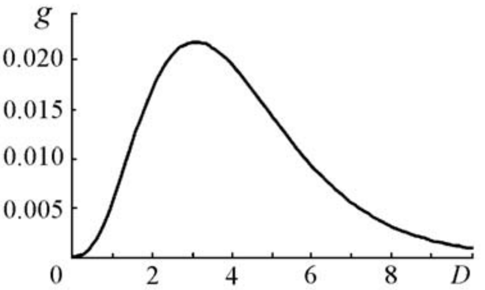

Fig. 4. Change in the pressure in the liquid p (1), in the rate of outflow of the vapor-water mixture u (2), and in the diameter of the cavitation bubbles D_1 (3) depending on the time. p, atm; u, m/s; D_1, μm; t, μs.

Fig. 5. Function of mass distribution of particles depending on their size. D, μm; g, %.

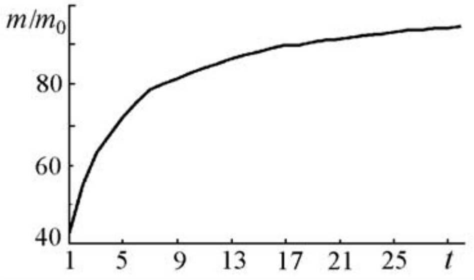

Fig. 6. Relative mass of the evaporated aerosol depending on the time, t, s.

p_m = 11.5 MPa for the ratio $S_2/S_1 = 0.3$ (the area of the clearance relative to the total area of the cross section of the atomizer tube): $u_1 = 53$ m/s; $u = 178$ m/s.

The time of outflow of the vapor-water mixture from the atomizer nozzle, determined from (20), comprises $t_{out} \approx 28 \cdot 10^{-3}$ s, which is larger than the time of propagation of the acoustic wave in the explosion chamber ($t = 6.7 \cdot 10^{-6}$ s). Thus, in the chamber, a vapor-water mixture with cavitation bubbles is formed within the first microseconds, and then this mixture outflows from the atomizer nozzle under pressure within several milliseconds.

Figure 4 shows dependences of the cavitation-bubble diameter, the pressure in the explosion chamber, and the velocity of the vapor-water mixture flow on the time of work of the atomizer. The pressure and the flow velocity will gradually decrease and the diameter of the vapor inclusions will grow with decrease in the flow rate of the vapor-water mixture. However, the dimensions of the inclusions will not exceed 240 μm (at p_f = 1.2 MPa).

In accordance with the algorithm described in Sec. 1.3, we obtain, using (10), (19), (21), and (23), the dependence of the relative mass of the drops on their diameter for our conditions and approximate it with the use of the particle-size distribution gamma function $f(x) = ax^{\alpha} \exp(-bx^{\beta})$. The parameters of such a distribution are as follows: $\alpha = 0, 1$; $b = 1$. The particle-size distribution mass function is related to the computational particle-size distribution function by the relation $g(x) = m/m_{10} f(x)$, where $m_{10} = \int\limits_0^{\infty} mf(xdx)$. The particle-size distribution mass function is presented in Fig. 5.

Thus, most of the drops obtained by the explosion-cavitation method have a diameter smaller than 5 μm and, for them, the evaporation determined by the curvature of their surface is essential. For the water aerosol, $\sigma = 0.0727$ N/m, $M = 18$ g/mole, $T = 293$ K, and $p_{pl} = 2486$ Pa. Using (27) and the gamma-distribution function parameters obtained earlier, we determined the dispergated-aerosol fraction evaporated during the course of 30 s. For example, drops with a diameter smaller than 1.54 μm (the mass fraction m/m_0 of such particles comprises 42%) evaporate in 1 s, particles with a diameter of 1.94 μm (m/m_0 = 55%) evaporate in 2 s, and so on. The calculation data obtained on the dynamics of the ratio between the final mass of a drop m and its initial mass m_0 are presented in Fig. 6.

Thus, even after 17 s, only 10% of the initial mass of the aerosol remains, and 90% of the liquid mass evaporates. This is in good agreement with the experimental data of [7]. According to the experimental data presented in Sec. 3, the measured aerosol concentration comprises 10% of the expected one (that could be attained in the case of uniform atomization of the initial liquid in the experimental chamber). It has also been established that the humidity in the experimental chamber increases after the atomization of the water in it.

Thus, an explosion atomization of a liquid makes it possible to obtain a microatomized aerosol, the larger part of which evaporates during the course of several seconds. The amount of evaporated liquid and the dispersion of the aerosol obtained can be changed by varying the parameters of the atomizer. Now the question arises of how the dispersion parameters and the concentration of the aerosol in the air will change with time.

2. Kinetics of a Dispersion Aerosol Cloud. *2.1. Assumptions used. Balance equation.* Thus, we have determined the initial size distribution of the liquid particles at the instant of explosion formation of an aerosol. In this case, the particle-size distribution gamma function has the following parameters: $\alpha = 0,\ 1$; $b = 1$.

We now consider the evolution of the particle-size distribution with time.

Following [9, 10], we write the balance equation (the integral variant of the Smolukhovskii equation) for the change in the particle-size distribution function with time. In this case, the following assumptions are used:

1) a cloud of particles is spatially homogeneous;

2) the effects of ultrasound, electrostatic, turbulent, and gravitational coagulation are disregarded (only the neglect of the gravitational coagulation might need clarification);

3) the vapor condensation is also disregarded (the time of this condensation is larger than the times considered by us);

4) pair collisions of particles are essential, and only the pair collisions are taken into account (the "packing" parameter, i.e., the ratio between the volume of all particles and the air volume occupied by it is much smaller than unity); in this case, each collision leads to the coalescence of particles. The evaporation due to the curvature of the surface of the drops having small sizes and their deposition on the walls of the experimental chamber are essential.

Thus,

$$\frac{\partial g(m, t)}{\partial t} = I_1 + I_2 + I_3 + I_4 . \tag{28}$$

Here I_1 defines the decrease in the number of drops with mass m in a unit volume during a unit time due to the collision of a drop with mass m with any drop with mass m':

$$I_1 = -g(m, t) \int_0^\infty K(m, m') g(m', t)\, dm' . \tag{29}$$

The term I_2 defines the appearance of particles of mass m due to the collisions of drops with a mass m' and drops with a mass $m - m'$:

$$I_2 = \frac{1}{2} \int_0^m K(m - m', m') g(m', t) g(m - m', t)\, dm' ,$$

the term I_3 defines the decrease in the mass of the drops due to their evaporation, and the term I_4 defines the decrease in the mass of the drops due to their precipitation.

2.2. Some suppositions on the kernel of the integral equation. Following [11], we will determine the probability of collisions of particles as a function of their masses: $K(m, m') = K_{\text{d}}(m + m')$, where $K_{\text{d}} = 6\cdot 10^3/\rho_{\text{liq}} \frac{1}{\text{s}\cdot\text{kg}}$.

In this case, the expressions for I_1 and I_2 will take the form

$$I_1 = -K_{\text{b}} g(m, t) \int_0^\infty (m + m') g(m', t)\, dm' ,$$

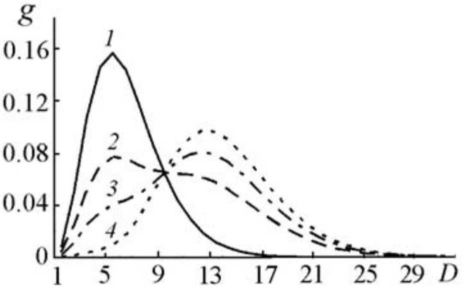

Fig. 7. Mass function of the particle-size distribution at t = 10 (1), 1000 (2), 3000 (3), and 6000 s (4). D, μm; g, %.

$$I_2 = \frac{K_b m}{2} \int_0^m g\,(m', t)\, g\,(m - m', t)\, dm' .$$

The sum of these terms is determined from the expression

$$I_1 + I_2 = K_b m \left[\frac{1}{2} \int_0^m g\,(m - m', t)\, dm' - g\,(m, t) \right] - K_b g\,(m, t)\, m_{\text{sum}}$$

(since $\int_0^\infty g(m', t)dm' = 1$, the total mass of the particles $m_{\text{sum}} = \int_0^\infty m' g(m', t)dm'$).

Figure 7 shows the calculated time dependence of the mass function of the size distribution of the aerosol particles, determined with account for their coagulation (the first two terms in Eq. (28)). The sizes of the aerosol particles increase with time; however, the rate of this increase decreases gradually, and the distribution function becomes constant within several hours (curve 4 in Fig. 7).

2.3. Estimation of the evaporation of aerosol particles. The term I_3 defines the decrease in the mass of the aerosol particles due to their evaporation (this term along with the term I_4 accounts for the fact that the total mass of the aerosol drops is not only redistributed but also decreases and that their size distribution function changes). The term I_3 is determined by the Maxwell equation for the mass of a particle:

$$I_3 = \frac{\partial}{\partial m} \left(\frac{dm}{dt} g\,(m) \right) = \frac{\partial}{\partial m} \frac{4\pi r D_{\text{dif}} M\,(p_{\text{d}} - p_{\text{pl}})\, g\,(m)}{RT} .$$

Using the Thomson (Kelvin) formula (26) and expressing the radius of a particle in terms of its mass, we obtain

$$I_3 = \frac{D_{\text{dif}} M \dfrac{\partial}{\partial m} \left(m^{1/3} g\,(m)\, (\exp \left(\dfrac{\sigma M}{RT m^{1/3} \rho_{\text{liq}}^{2/3}} \right) - 1) \right)}{RT \rho_{\text{liq}}^{1/3} p_{\text{pl}}} .$$

2.4. Estimation of the precipitation of water drops. We now will estimate the influence of the gravitational precipitation of submicron-aerosol particles on the kinetics of its cloud. For this purpose, the dependence of the linear rate of precipitation of an aerosol on the time, the radius of its particle, and the other parameters of the system will be determined. To obtain such a dependence, it is necessary to determine the forces acting on an aerosol drop: the gravity force and the drag force. Then

$$m\dot{u}_{\text{d}} = mG - 6\pi r \eta_0 u_{\text{d}} , \qquad (30)$$

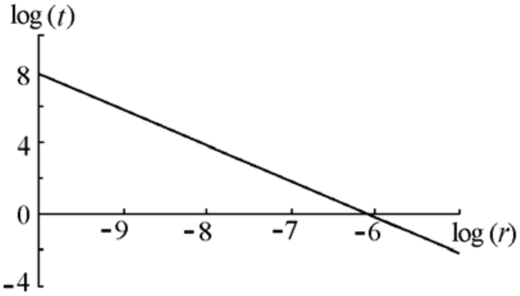

Fig. 8. Dependence of the time of precipitation of water drops on their radius. *r*, m; *t*, min.

where the second term on the right side of the equation defines the Stokes force of viscous friction. The solution of Eq. (30) has the form $u_d = \frac{4G\rho_{liq}}{9\eta_0}r^2\left(1 - r\sqrt{\frac{2\rho_{liq}}{9\eta_0 G^2 t + 2\rho_{liq}r^2}}\right)$. However, in the case of microatomized water aerosols in the air, the second parenthetical term can be disregarded and, therefore, the motion of an aerosol drop under the gravity and friction forces can be considered as uniform.

We now estimate the time of precipitation of water drops having different sizes in the air under the gravity force at normal conditions. Figure 8 shows, in the logarithmic scale, the dependence of the time of precipitation of such drops per implies one meter on their radius.

Our calculations have shown that only the drops with a radius larger than 1 μm precipitate rapidly: the precipitation time is 0.69 min for r = 10 μm and 116 h for r = 0.1 μm. Thus, for submicron aerosols, the precipitation should be taken into account only in the case where the time measured by hours and not by minutes is of interest. Nevertheless, the term accounting for the rate of gravitational precipitation will have the form

$$I_4 = \frac{\partial}{\partial m}\left(u_d(m)\,g(m)\right) = \frac{\partial}{\partial m}\left(\frac{G\rho_{liq}}{3\eta_0}\left(\frac{4}{3}\right)^{1/3}\left(\frac{m}{\pi}\right)^{2/3} g(m)\right).$$

An aerosol is produced by the explosion method in the case where an explosive is positioned at the bottom of the explosion chamber. The velocity of ejection of the liquid from the nozzle of the atomizer u_0 is of the order of 180 m/s, and the horizontal component of the velocity vector is, as a rule, insignificant; therefore, drops will precipitate mainly on the ceiling of the explosion chamber due to their flying apart.

The only force acting on a drop in the process of its flying to the ceiling is the Stokes friction force. Therefore,

$$m\dot{u}_d = -6\pi r\eta_0 u_d\,, \tag{31}$$

$$u(0) = u_0\,.$$

Solving Eq. (31), we obtain $u_d = 3\sqrt{\frac{\eta_0 u_0}{4\rho r^2 u_0 t + 9\eta_0}}$. Integration of the latter equation gives the expression for the precipitation time

$$t_{pr} = \frac{\left(\frac{H}{6\rho_{liq}r^2 u_0\sqrt{\eta_0 u_0}} - 3\sqrt{\eta_0}\right)^2}{4\rho_{liq}r^2 u_0} - 9\eta_0\,.$$

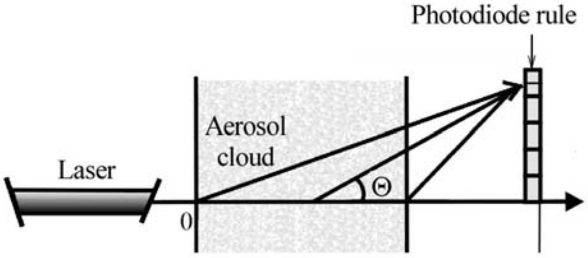

Fig. 9. Scheme of interaction of radiation with an aerosol.

Our estimates show that the drops with a radius of 10 μm or smaller practically never reach the ceiling of the chamber ($t_{pr} \sim 10^{11}$ h), and they can precipitate on it only due to the Brownian coagulation. However, it is necessary to take into account the fact that aerosol drops move not separately but in a flow, and the drops in the front of the flow will primarily experience a friction, which sharply increases the probability of their collisions. In the spatially homogeneous formulation, this phenomenon can be estimated by determining the kernel function in the coagulation equation. For example, the time dependence of the function $K(m, m')$ can be considered: the probability of collisions of particles is higher at the first instants of formation of an aerosol and the coagulation becomes Brownian at the instant the motion of the drops is retarded.

Thus, the fourth term on the right side of Eq. (28) is essential only in the case of fairly large times and only in the gravitational-precipitation sense. The third term of this equation, on the contrary, is essential in the case of small times, where the particles are still small (are not subjected to coagulation) and the evaporation of them is due to the curvature of their surface.

3. Experimental Methods for Measuring the Dispersity of Aerosols. *3.1. Optical method for measuring the dispersity of aerosols with micron-size particles.* Contactless optical methods based on the solution of direct and reverse problems of aerosol optics are widely used for measuring the spectrum of micron-size particles in two-phase media. One such method is the method of small-angle scattering based on recording of the light scattered by particles at small angles to the initial direction of propagation of the probe radiation [12] (Fig. 9). This method is used on the assumption that the particles being considered are spherical and multiple scattering is absent because of the small concentration of the particles.

In the present work, we used a modified method of small-angle scattering based on the determination of the particle-size distribution function by solving a series of direct problems of aerosol optics. [13]. The essence of this method is that the sizes of aerosol particles are determined on the basis of the measured small-angle scattering indicatrix by exhaustion of the corresponding parameters of the distribution function. The gamma distribution was used as a basis function.

The measuring laser complex comprises an emitter, a photodetector unit, and a recording-apparatus unit. An LG-78 helium-neon laser with a radiation wave length of 0.63 μm was used as an emitter. The radiation of this laser passed through a diaphragm and, in doing so, was subjected to a 40-Hz frequency modulation for exclusion of the external radiation background.

To record the radiation scattering in the range of angles $\Theta = (0 - 15)^{\circ}$, we used silicon FD-24K photodiodes, of which a photodiode rule including seven radiation detectors was formed. The signals from the photodiodes were recorded by a computer equipped with a high-speed L-783 digitizer of the L-Card firm with a digitization frequency of 285 kHz for each channel.

3.2. Scheme of a measuring stand. To perform measurements, we have developed and fabricated a special experimental measuring stand, the structural scheme of which is presented in Fig. 10. The velocity of ejection of aerosol particles was measured with the use of a high-speed VideoScan/C/G4 (VideoScan) camera with a recording rate of 500–10,000 frames/s and an exposure from 50 μs to 2 ms. The heat fields of an aerosol cloud were recorded by a contactless method with the use of a ThermoPro-TP8 infrared imager (Guide Infrared Technology Co.) with a measurement range from -20°C to $+800^{\circ}$C and a frame frequency of 50 Hz. The pressure in the combustion chamber was measured by an RZMA pressure transducer (HBM, Germany).

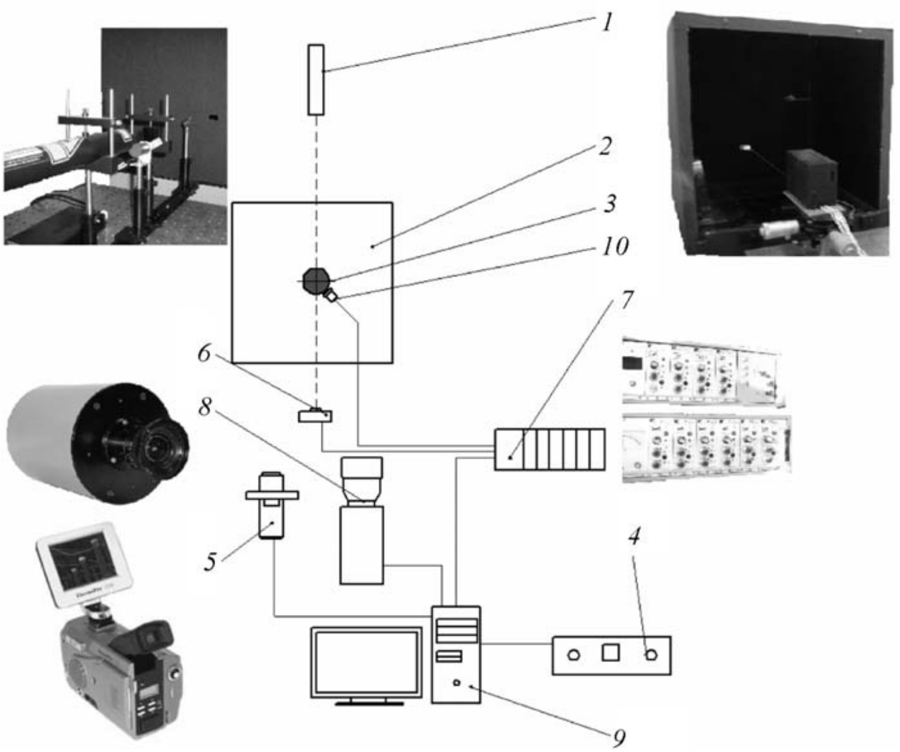

Fig. 10. Diagram of an experimental measuring stand: 1) laser; 2) measuring volume; 3) explosion generator of an aerosol; 4) activation pulpit; 5) video camera; 6) photodiode rule; 7) KWS multichannel amplifier; 8) infrared imager; 9) automatic regulator of power; 10) pressure transducer.

The dispersion characteristics of an aerosol of volume 1 m^3 were recorded by the above-described method (Fig. 10). In addition, the method of sampling was used, and the dispersity of the sample was measured with the use of a PIP-9.0 optical analyzer of particles (Olympus) with a maximum resolution of 1000× and a GSM-840 scanning electron microscope with a measurement limit of 100 nm.

4. Results of Experimental Investigations. *4.1. Particle-size distribution mass function.* An LID-2M optical measurement complex has been developed for control of the dispersivity of an aerosol [13]. Its operation is based on the use of the method of small-angle scattering of radiation with a wavelength of 0.63 μm by aerosol particles of size from 1 to 100 μm. A further modernization of the method has made it possible to measure the concentration of an aerosol in a definite volume, with the result that new data on the aerosol composition were obtained: a substantial decrease in the mass of the atomized liquid was detected in the visible part of the field. It was suggested that the "invisible" part of the aerosol field contains particles of diameter smaller than 1 μm that are inaccessible for measuring by the LID-2M complex.

The study of classical literature sources (works of Maxwell, Thomson, and Einstein) allowed us to realize that the loss in the mass of a liquid (water in our experiments) is caused, first of all, by its rapid evaporation due to the surface curvature of the particles with a diameter smaller than 1 μm. Calculations of the dependence of the lifetime of the aerosol particles on their diameter have shown that, for pure water, this time ranges from 10^{-8} to 10^{-2} s. The evaporation of water increases the humidity in the region of atomization of an aerosol. Psychrometric investigations have shown that the humidity of the medium increases in accordance with the decrease in the mass of the atomized water.

In the present work, we experimentally investigated the genesis of a dispersed aerosol, the influence of the impurities hindering the evaporation and the impurities making possible the recording of nanodimensional liquid particles in the aerosol field on the formation of dispersed particles, and the influence of the viscosity of a liquid on the process of its atomization.

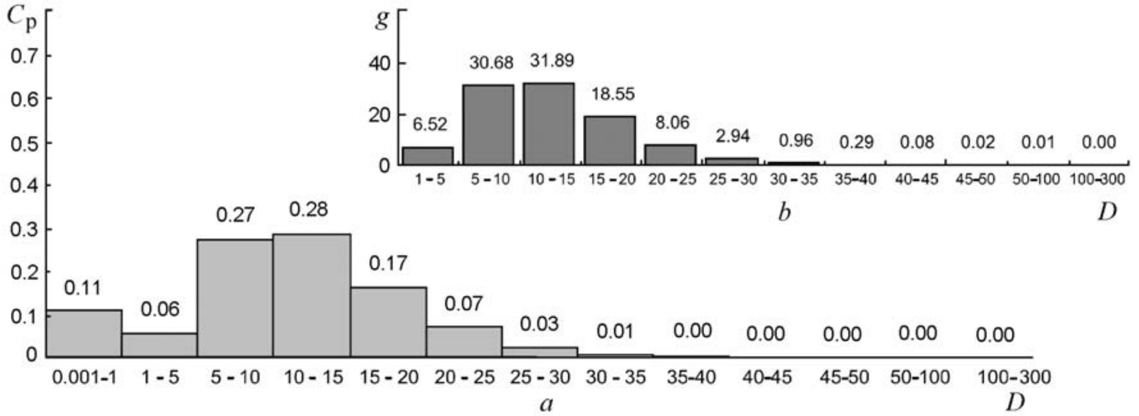

Fig. 11. Concentration and mass distributions of the particles in an aerosol depending on their size at $t = 1$ s: a) histogram of the concentration distribution of the particles in the presence of vapor; b) mass distribution of the particles with a diamete ofr more than 1 μm. C_p, g/m^3; D, μm; g, %.

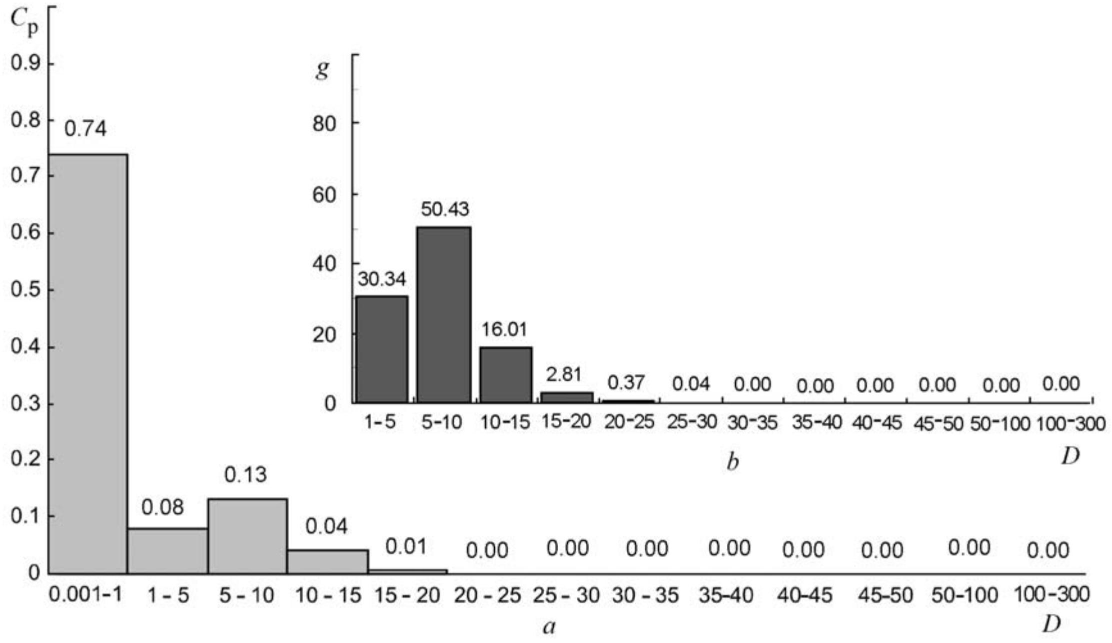

Fig. 12. Concentration and mass distributions of the particles in an aerosol depending on their size at $t = 3$ s. The designations a and b are identical to those in Fig. 11. C_p, g/m^3; D, μm; g, %.

Data on the evolution of a water aerosol containing 10% NaCl (the liquid mass is 1 g) obtained with the use of the LID-2M apparatus are presented in Figs. 11–13. It follows from these figures that the process of filling of a closed space of volume 1 m^3 with an aerosol finishes practically within 3–6 s.

The rapid changes in the mass distribution of the aerosol particles within the first 2–3 s point to the fact that the mechanism of formation of the aerosol field is complex in character and depends on the gasdynamics of the flow generated by the combustion of the explosive, on the diffusion of the aerosol particles, and, especially, on the evaporation of these particles. However, this process stabilizes within 3–6 s. A successive consideration of Figs. 11–13 additionally supported the conclusion that the evaporation plays a large role in the formation of an aerosol. These figures also show that the fractions of the water vapor and of the submicron particles increase gradually due to the evaporation of water from the aerosol drops and the decrease in the micron-size particles.

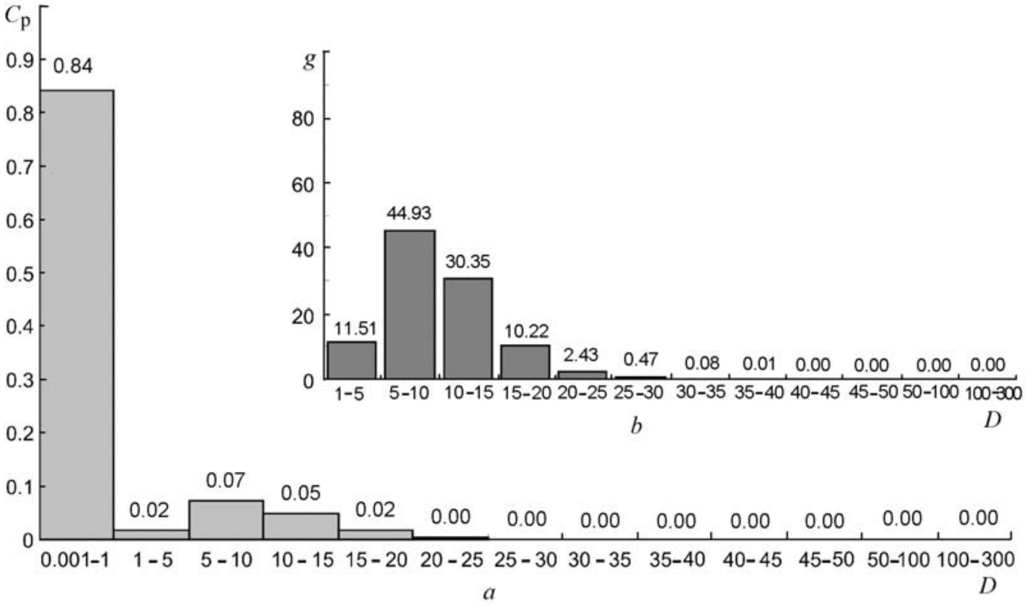

Fig. 13. Concentration and mass distributions of the particles in a water aerosol depending on their size at $t = 6$ s. The designations *a* and *b* are identical to those in Fig. 11. C_p, g/m^3; *D*, μm; *g*, %.

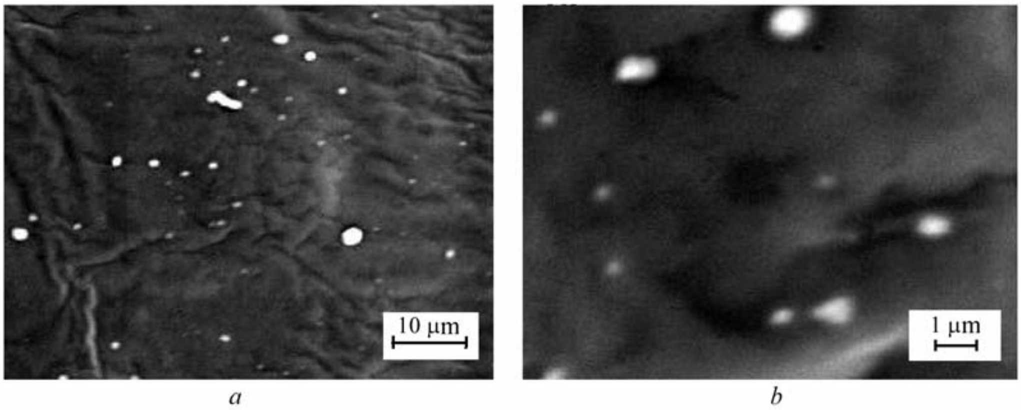

Fig. 14. Traces of particles in the aerosol of an aqueous solution of NaCl: ×1000 (a) and ×5000 (b).

4.2. Presence of nanodimensional particles in an aerosol. The concentration of the submicron-aerosol part (0.001–1 μm) was determined as the difference between the mass of the atomized water-containing liquid and the liquid mass measured on the LID-2M setup. Our psychrometric investigations have shown that this part of the aerosol correspondingly increases the humidity of the medium. However, the psychrometer gave a result within 10–20 min after the generation of the aerosol. In accordance with the physical-mathematical model (part 1), in the initial period of formation of an aerosol in the process of explosion atomization of a liquid, a wide variety of dispersed particles — from the molecular and nanodimensional particles to the micron ones — is formed. To show that nanoparticles are formed at the initial instant of time, the products of atomization of aqueous solutions of NaCl and of mixtures containing additions of nanodimensional diamond particles were investigated. Such mixtures allow one to detect a trace of the water-containing particles because the water particles of size smaller than 1 μm evaporate in 10^{-7}–10^{-2} s.

Figures 14 and 15 show results of investigations carried out with the use of an electron microscope. Samples were taken directly from a spray cone. The results obtained point to the fact that the indicated particles exist. However, the electron microscope used failed to visualize the trace of particles of size smaller than 200 nm.

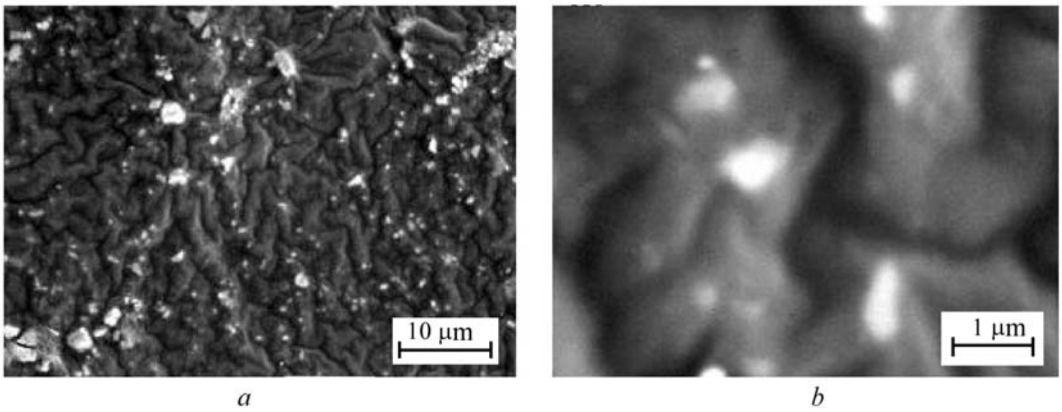

a *b*

Fig. 15. Traces of particles in the aerosol of a water suspension containing diamond particles of average size 4 nm: ×1000 (a) and ×5000 (b).

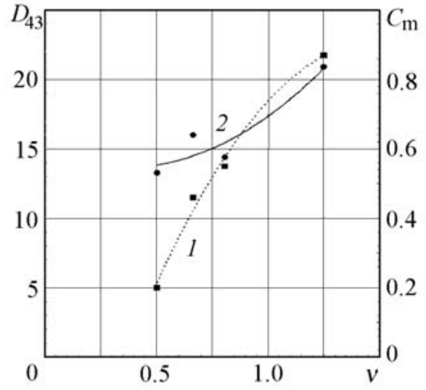

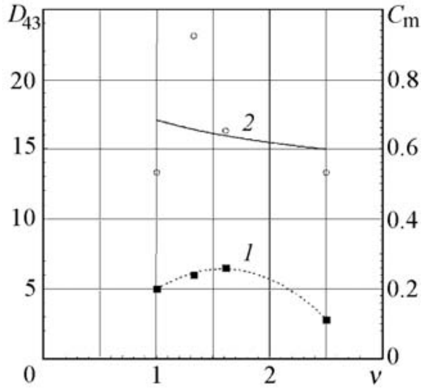

Fig. 16. Dependence of the concentration C_p (1) and the average diameter of the particles D_{43} (2) in the aerosol of an aqueous solution of glycerin on its viscosity. C_p, g/m^3; D_{43}, µm; ν, cP.

Fig. 17. Dependence of the concentration C_p (1) and the average diameter of the particles D_{43} (2) in the aerosol of an aqueous solution of ethyl alcohol on its viscosity. C_p, g/m^3; D_{43}, µm; ν, cP.

4.3. Influence of the viscosity of a liquid and of impurities on the average size of the aerosol particles. We investigated the dependence of the average size D_{43} of the aerosol particles and their concentration on the viscosity of a dispergated liquid (Figs. 16 and 17). The initial viscosity was obtained by preparation of a mixture of water with glycerin and a mixture of water with ethyl alcohol. In this case, the viscosity varied near the average values: $\nu = 1.5$ cP (Fig. 16). These investigations have shown that the impurities in aqueous solutions determine the lifetime of the aerosol drops.

It has been established experimentally that, in the majority of cases, the aerosol particles are not evaporated completely because of the presence of foreign impurities in them [14]. The density of the vapor over the surface of a drop ρ_d in a solution depends on the mole fraction η of the liquid that changes during the evaporation of the liquid because the concentration of the substance dissolved in a drop changes with change in its radius. The rate of evaporation of a liquid drop is determined with account for the influence of an impurity on this process from the following expressions [15]:

$$I = 4\pi r D_{\mathrm{dif}} \frac{(\eta \rho_{\mathrm{d}} - \rho_{\mathrm{pl}})}{M}, \tag{32}$$

TABLE 1. Time of Complete Evaporation of Water from the Drops of the 20% Solution of NaCl

r_{in}, μm	r_{f}, μm	t_i, s	
		20% solution of NaCl	Pure water
100	45	17	6.75
50	22	3.85	1.72
40	18	2.44	1.12
30	13	1.32	0.63
20	9	0.68	0.33
15	7	0.42	0.18
10	4	0.2	0.09
5	2	0.04	0.01

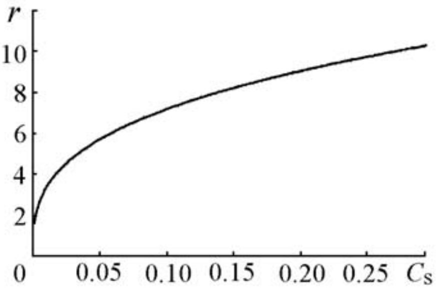

Fig. 18. Dependence of the radius of a drop of a sodium-salt solution on the relative concentration of the salt in the solution. r, μm; C_{s}, g/m^3.

$$\eta = \frac{\dfrac{1}{M_{\text{lq}}(1 - C_{\text{s}})}}{\left(\dfrac{C_{\text{s}}}{M_*} + \dfrac{1 - C_{\text{s}}}{M_{\text{lq}}}\right)} . \tag{33}$$

For comparison of the influence of substances with different molecular masses on the rate of evaporation of water drops, we determined the influence of the content of sodium salt (molar mass 52 g/mole) and glycerin (molar mass 92 g/mole) on the evaporation of these drops. Our calculations have shown that a dissolved impurity can substantially influence the evaporation, and the larger the molar mass of a substance, the larger the decrease in the evaporation rate.

The influence of the content of an impurity on the final size of the aerosol drops was estimated with the use of the expression for determining the change in the radius of an aerosol drop with account for the change in the impurity concentration, obtained by rearrangement of Eq. (32):

$$\frac{dr}{dt} = \frac{D_{\text{dif}}}{r\rho_{\text{liq}}} \frac{(\eta(t)\rho_{\text{d}} - \rho_{\text{pl}})}{M} . \tag{34}$$

The time during which the evaporation is completed and the final size of the drops were calculated from the condition $\frac{dr}{dt} \to 0$. Calculations were carried out for an NaCl solution. The results of calculations for the water aerosol obtained from the NaCl solution are presented in Table 1. It should be noted that the influence of the crystallization of the salt on the physicochemical and thermodynamic state of an aerosol drop was not taken into account.

The content of the salt in a solution was selected in accordance with its approach to the maximum-solubility limit (37%) and the adequate decrease in the initial sizes of the aerosol particles, which made it possible to determine the characteristics of the aerosol with the use of the available methods for determining the dispersion characteristics of

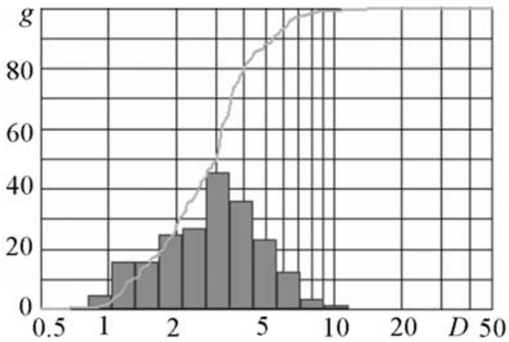

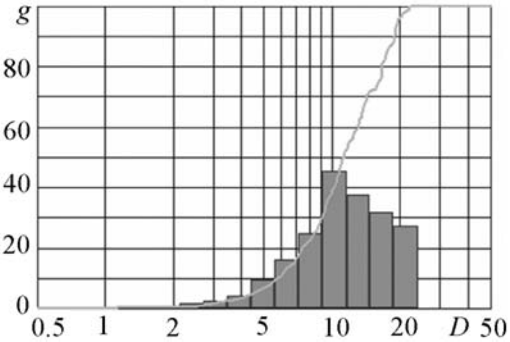

Fig. 19. Results of measurement of the mass distribution of the particles in the aerosol obtained from the 20% solution of NaCl depending on their size. *g*, %; *D*, μm.

Fig. 20. Calculated mass distribution of the particles in the aerosol obtained from the 20% solution of NaCl depending on their size. *g*, %; *D*, μm.

substances. The degree of decrease in the size of the aerosol particles because of their evaporation was estimated by the equation

$$r = r_0 \sqrt[3]{\frac{\eta\rho_{\text{liq}}}{\rho_{\text{imp}}}}\,. \tag{35}$$

Results of determining the decrease in a 20-μm drop of a sodium-salt solution are presented in Fig. 18. Figure 19 presents results of measuring the diameter of the aerosol drops of the sodium-salt solution obtained by the sampling method with the use of an optical analyzer (microscope). The initial dispersity of the aerosol can be determined by the measurement results with the use of (35). Results of such calculations are presented in Fig. 20.

In [16], it has been experimentally shown that initially the drops evaporate rapidly and then the rate of evaporation decreases. It has been possible to follow the evaporation of individual water drops of micron size for 3–4 h. This exceeds the theoretical lifetime of a drop by many times. One reason for the anomalously long evaporation is the ability of water to adsorb carbon dioxide. On the surface of a drop, the concentration of carbon-dioxide molecules increases, the concentration of water molecules decreases, and, correspondingly, the mole fraction of water decreases with decrease in the rate of its evaporation (Eq. (32)).

It has been established in [17] that the diffusion of vapor from the surface of large drops (of size larger than 100 μm) decreases by 22%, which, in accordance with Eq. (32), substantially influences the evaporation rate.

Thus, it has been established theoretically and experimentally that the viscosity of a liquid and the impurities in it influence the rate of evaporation of the aerosol drops; in this case, the impurities exert a maximum influence on the evaporation from the surface of curves, and the larger the surface curvature, the larger this influence, which agrees with the classical results [18].

Conclusions. Results of theoretical and experimental investigations of the generation of a liquid-drop aerosol by the explosion method and of the further evolution of this aerosol are presented. The investigations of the genesis of a water aerosol and of the mechanisms of evaporation of the aerosol particles allowed the following conclusions:

1) in the process of explosion generation of a liquid-drop aerosol, of great importance is the cavitation of the liquid; under conditions favorable for the cavitation, a maximum dispersion of the aerosol can be attained, which is important for the solution many practical problems.

2) a mathematical model of explosion generation of an aerosol, the results of calculations with which agree with the experimental data, has been developed; this model allows one to select the characteristics of an atomizer such that an aerosol with definite dispersion parameters be obtained;

3) the processes of further evolution of the aerosol obtained were theoretically investigated with account for the evaporation, coagulation, and precipitation processes.

A series of experiments on the explosion atomization of liquid aerosols was conducted with the use of a specially developed measuring complex. The following results have been obtained.

1. The mass distribution of the particles of an aerosol stabilizes in the volume occupied by it within 3–6 s.

2. Because of the rapid evaporation of water from the particles of size less than 1 μm (during the time 10^{-7}–10^{-2} s), the main part of the aerosol (more than 50%) represents submicron particles, a cold vapor formed as a result of the evaporation of submicron particles, and a cavitation liquid present primarily in the aerosol (~20% of this liquid represents vapor and submicron particles — the contents of the cavitation bubbles).

3. It has been established that weakly evaporating impurities, such as glycerin and sodium salt, decelerate the evaporation of particles from a water aerosol. A technique making possible the use of the explosion atomizer developed for dispergation of various substances and mixtures of them with account for their physicochemical properties has been developed.

The authors express their thanks to researchers at the Institute of Problems of Chemical and Energy Technologies: Doctor of Chemical Sciences S. G. Il'yasov for developing the explosive used in our experimental investigations; Doctor of Technical Sciences A. A. Pavlenko for valuable observations concerning the results of the work; Chief Engineer of the Federal Scientific-Production Center "Altai" N. V. Bychin for the electron-microscopy results.

NOTATION

a, b, parameters of the particle-size distribution gamma function $f(x)$, dimensionless; c, velocity of sound in the liquid, m/s; c_0, velocity of sound in the air, m/s; C_p, concentration of particles in an aerosol, g/m^3; C_s, concentration of an impurity in a solution; c_V, specific heat of a gas at constant volume, J/kg/K; D, diameter of an aerosol drop (particle), μm; D_1, diameter of a vapor inclusion (cavitation bubble), μm; D_2, diameter of a cavitation element (a cavitation bubble and the liquid layer surrounding it), μm; D_3, diameter of a vapor inclusion (cavitation bubble) after its expansion to the atmospheric pressure, μm; D_4, diameter of a vapor element (a cavitation bubble and the liquid layer surrounding it) after the expansion to the atmospheric pressure, μm; D_{43}, mean-mass diameter of drops (particles), μm; D_{dif}, diffusion coefficient, m^2/s; $G = 9.81$, free-fall acceleration, m/s^2; h, minimum thickness of the water layer of a cavitation element, μm; H, height of the experimental chamber, m; I, intensity of the wave field, J/s/m^2; i, number of a liquid layer; I_1, I_2, I_3, I_4, terms of the Smolukhovskii balance equation, 1/s; $k = V_{\text{liq}}/V$, cavitation index; $K(m, m')$, probability of collision of drops with masses m and m' in a unit time, 1/s; K_d, probability coefficient of collision of drops, 1/s/kg; L, thickness of a liquid layer, cm; M, molecular weight of a liquid drop, g/mole; m, mass of particles of diameter x, g; M_*, molecular wight of an impurity, g/mole; m_{10}, arithmetic-mean mass of particles, g; m_g, mass of the gas products of the explosive reaction, g; M_{sol}, molecular weight of a solvent, g/mole; m_{sum}, total mass of drops, g; M_{liq}, mass of the atomized liquid, g; N, number of liquid layers; n_i, number of particles in the liquid layer i; n_{rel}, relative number of particles; p, pressure, MPa; p_a, atmospheric pressure, atm; p_0, pressure in the environment, MPa; p_d, partial pressure above a drop, MPa; p_f, final pressure in the combustion chamber after the explosion; p_m, pressure amplitude of an acoustic wave in the liquid, MPa; p_{pl}, partial pressure above a plane surface, MPa; Q, energy of the explosion transformation released as a result of the discharge initiation, J; r, radius of a drop, μm; $R = 8.314472$, universal gas constant, m^2·kg/s^2/K/mole; r_0, initial radius of a drop prior to its evaporation, μm; S_1, area of the cross section of a water tunnel, cm^2; S_2, area of the atomizer hole, cm^2; t, time, s; T, absolute temperature, K; T_g, temperature of the gases released as a result of the explosive action, K; t_{life}, lifetime of a drop, s; t_{pr}, time of precipitation of drops, s; t_w, time of travel of a sound wave in a liquid layer, s; t_{out}, time of outflow of a vapor-water mixture through the atomizer hole, s; u, velocity of the drops at the output of the atomizer nozzle, m/s; u_1, velocity of movement of the vapor-water mixture in the atomizer, m/s; u_d, velocity of movement of a drop, m/s; $\dot{u}_d$, acceleration of movement of a drop, m/s^2; ΔU, change in the internal energy of a gas, J; V, volume of a liquid, cm^3; V_1, volume of the explosion chamber, cm^3; V_{el}, volume of a cavitation element (a bubble and the liquid surrounding it), cm^3; V_{liq}, volume of the liquid in a cavitation element, cm^3; x, variable particle-size distribution function; Z_m, maximum displacement of particles in a wave, μm; Z_{ef}, effective thickness of a plane discontinuity, μm; α, β, parameters of the gamma-distribution function $f(x)$; γ, adiabatic index of the detonation products; η, mole fraction of the liquid, ratio between the amount of the dissolved substance and the total amount of the substance in a solution; η_0, kinematic viscosity of the air, m^2/s; λ, length of a sound wave, μm; ν, viscosity, cP; ρ_0, density of the air, kg/m^3; ρ_{liq}, density of the liquid, kg/m^3; ρ_d, density of the vapor over the surface of a drop, kg/m^3; ρ_{pl}, density of the vapor over a plane surface, kg/m^3; ρ_{imp}, density of the impurity in a solution, kg/m^3; σ, surface tension coefficient, N/m; ω, vibration frequency, Hz. Subscripts: m, maximum; g, gas; w, wave; el, element; ef, effective; out, outflow; rel, relative; f, final; d, drop; pl, plane; sum, summary; pr, precipitation; s, salt; sol, solvent; imp, impurity; a, atmospheric; in, initial; liq, liquid; p, particle.

REFERENCES

1. V. M. Burenok, V. Yu. Korchak, and S. S. Smirnov, Nonlethal weapon — a constituent of the future armament, *Vestn. Akad. Voen. Nauk*, No. 4, 117–127 (2007).
2. A. A. Onishchuk, T. G. Tolstikova, I. V. Sorokina, A. M. Baklanov, A. A. Karasev, V. V. Boldyrev, and V. M. Fomin, Effect of indometacin nanoparticles deposited in lungs (production of nanodimensional aerosol forms of medicinal preparations weakly soluble in water), *Dokl. Ross. Akad. Nauk*, **425**, No. 5, 692–695 (2009).
3. V. I. Malyshev, The concept of complex concealment and preservation of objects needed for stable functioning of economics and survival of population at war time (project), *A Volume of Publications of the Center of Strategic Investigations of Civil Defense*, Issue 14, CSICDMEE of Russia, Moscow (1999), pp. 53–74.
4. S. V. Stebnovskii, Pulsed dispergation of a liquid volume as the limiting regime of its destruction, *Fiz. Goreniya Vzryva*, **44**, No. 2, 117–128 (2008).
5. V. K. Kedrinskii, *Gas Dynamics of Explosion: Experiment and Models*, Izd. SO RAN, Novosibirsk (2000).
6. I. F. Kobylkin, V. V. Selivanov, V. S. Solov'ev, and N. N. Sysoev (Eds.), *Shock and Detonation Waves. Methods of Investigation* [in Russian], 2nd rev. augm. ed., Fizmatlit, Moscow (2004).
7. B. I. Vorozhtsov, O. B. Kudryashova, and V. A. Arkhipov, Simulation of the process of dispergation of a liquid in an explosion gas generator, *Izv. Vyssh. Uchebn. Zaved., Fizika*, **51**, No. 8/2, 107–114 (2008).
8. R. I. Nigmatulin, *Dynamics of Multiphase Media* [in Russian], in 2 parts, Pt. 1, Nauka (Edit. Office of Phys. Mat. Liter.), Moscow (1987).
9. L. S. Ivlev and Yu. A. Dovgalyuk, *The Physics of Atmospheric Aerosol Systems* [in Russian], NIIKh SPbGU, St. Petersburg (1999).
10. V. M. Voloshchuk, *Kinetic Theory of Coagulation* [in Russian], Gidrometeoizdat, Leningrad (1984).
11. A. M. Golovin, On the problem of solving the coagulation equation for rain drops with allowance for their condensation, *Dokl. Akad. Nauk SSSR*, **148**, No. 6, 1290–1293 (1968).
12. V. A. Arkhipov and V. F. Trofimov, Characteristics of a centrifugal injector spray jet under nonstandard conditions, *Aviatsionnaya Tekh.*, No. 1, 70–72 (2003).
13. I. R. Akhmadeev, *Method and Quickly Acting Laser Facility for Investigating the Genesis of a Technogenic Aerosol by the Scattering of a Beam in a Controlled Volume*, Author's Abstract of Candidate's Dissertation (in Engineering), Biisk (2008).
14. K. Spurnyi, Ch. Nekh, B. Sedlachek, et al., *Aerosols* [Russian translation], Atomizdat, Moscow (1964).
15. A. N. Ishmatov and B. I. Vorozhtsov, Investigation of the development of a microatomized liquid aerosol with allowance for the influence of a poorly evaporating admixture, in: *Brief Communications in Physics* [in Russian], No. 1, FIAN, Moscow (2010), pp. 22–27.
16. N. Gudris and L. Kulikowa, Die Verdumpfung Keiner Wasser Tropfen (Evaporation of small drops of water), *Zeitschrift für Physik*, **25**, No. 2, 121–132 (1924).
17. E. R. Altwicker and C. E. Lindhjem, Absorption of gases into drops, *AIChE J.*, **2**, No. 34, 329–332 (1988).
18. N. A. Fuks, *Evaporation and Growth of Droplets in a Gaseous Medium* [in Russian], Mir, Moscow (1986).